Sensitivity analysis and optimization of vibration modes in continuum systems

Akihiro Takezawa[a,*], Mitsuru Kitamura[a]

[a] *Division of Mechanical Systems and Applied Mechanics, Faculty of Engineering, Hiroshima University, 1-4-1 Kagamiyama, Higashi-Hiroshima, Hiroshima, Japan*

Abstract

The sensitivity analysis of objective functions including the eigenmodes of continuum systems governed by scalar Helmholtz equations is carried out in continuum form. In addition, based on the sensitivity, the mode shapes are specified through numerical optimization. Using the continuum sensitivity and adjoint equation, the physical nature of them can be analyzed, which helps to explain the nature of the target optimization problem. Moreover, the continuum sensitivity and adjoint equation contribute to the quick numerical implementation of sensitivity analysis using software that can solve an arbitrary partial differential equation directly. A scalar Helmholtz equation in 1D or 2D domain is considered. The sensitivity analysis is performed for the general objective function formulated as a function of the eigenmode in continuum form. A minimization problem using the least squared error (i.e., difference) between the eigenvector and target mode shape is set as a sample objective function for both the first and second eigenmodes. The sen-

*Corresponding author. Tel: +81-82-424-7544; Fax: +81-82-422-7194

Email addresses: akihiro@hiroshima-u.ac.jp (Akihiro Takezawa), kitamura@hiroshima-u.ac.jp (Mitsuru Kitamura)

sitivity and the adjoint equation are derived for this objective function. 1D and 2D numerical sensitivity analysis and optimization examples are studied to illustrate the validity of the derived sensitivity.
Keywords: Sensitivity analysis, Eigenmode, Helmholtz equation, Optimal design, Finite element method

1. INTRODUCTION

The dynamic characteristics are one of the most important sets of properties in mechanical devices. To design devices with specified dynamic characteristics, various numerical optimization techniques were proposed in the context of a structural optimization field. In terms of the mechanical vibration, the most fundamental design specification is to avoid external disturbance vibrations resonating in the device. The fundamental method of achieving this is to maximize the lowest eigenfrequency. Starting from the early work in conventional shape optimization and grillage layout optimization [1, 2], the homogenization or solid isotropic material with penalization (SIMP) based topology optimization [3, 4] was applied to the problem [5, 6, 7, 8, 9]. Moreover, it was studied in various structural optimization methodologies as a benchmark problem [10, 11, 12, 13]. Specifying an eigenfrequency for the target value [14] is also an effective way of avoiding resonance. Another approach for optimizing the response against an external dynamic load is the optimization of output displacement based on frequency response analysis [15, 16, 17, 18] or time transient response analysis [19, 20, 21]. The maximization of the gap of the eigenfrequencies is also an interesting branch of the eigenfrequency optimization [10, 22].

Eigenmodes are also an important factor in the optimization of vibration characteristics. For example, as proposed in [7], the eigenmode shape is used to track the desired vibration during the optimization entailing eigenmode switching based on the modal assurance criterion (MAC). Moreover, aside from the above work, which regards vibration as a phenomenon to be avoided, some research has proposed the optimization methodology of the vibration resonators that uses vibrations for the mechanical function [23, 24, 25, 26]. In this type of resonator, the eigenmode that dominates the shape of deformation against the external periodic load is an important design factor in addition to the resonance frequency. Some research had difficulty with the optimization of the shape of the vibration mode [25, 27, 28]. Their approach was based on the discretization of the original continuum problem to a discrete problem using the finite element method (FEM). This discretization enabled the optimization of eigenmodes based on the eigenvector sensitivity analysis of matrices [29, 30, 31].

The concept of sensitivity analysis is not limited to discrete systems. As treated in some textbooks, the sensitivity and adjoint equations can be derived in the form of a continuum (e.g., [32, 33, 34, 35, 36]). This is the fundamental sensitivity analysis of continuum systems independent of discretization using numerical methods. By performing the sensitivity analysis in continuum form, an adjoint equation similar to the state equation can be obtained. Using this equation, the physical sense of the sensitivity and the adjoint equation can be analyzed as in [36]. This must be helpful for researchers and engineers studying the nature of vibration optimization. Moreover, in some commercial or open-source software, an arbitrary partial

differential equation can be directly solved numerically by writing the PDE directly in the software [37, 38]. If the adjoint equation is derived in continuum form, it can be directly solved using such software without self-produced code. Thus, it is necessary to broaden the design freedom of devices using external excitation vibrations. However, to the best of the authors' knowledge, sensitivity analysis in continuum form for the optimization problem of eigenmodes of continuum systems was studied only by [39]. In [39], the adjoint variable is calculated through modal analysis. Thus, the derivation of eigenmode sensitivity requires eigenfrequencies and eigenmodes that are of higher order than the target eigenfrequencies and eigenmodes. This must increase the computational cost of the optimization simply for solving the adjoint equation.

In this research, we derive the continuum sensitivity of the objective function including the eigenmodes of continuum systems governed by the scalar Helmholtz equations without using a modal method. Numerical optimization for the simple 1D and 2D vibration problems are also performed. That is, a scalar Helmholtz equation in the 1D or 2D domain is first considered. Then the sensitivity analysis is performed according to the procedure shown in [36]. A sample objective function is set as a minimization problem of the least square error of the first or second eigenvector and the target function. For this objective function, the sensitivity and the adjoint equation are derived in continuum form. The simple 1D string and 2D membrane vibration problems are set as numerical examples. The Helmholtz equation and the adjoint equation are solved numerically using the FEM for these problems. The sensitivity is calculated using the obtained state and adjoint variables.

The results are compared with the sensitivity derived by the finite difference method to illustrate the validity of the derived sensitivity. Finally, some optimization problems are solved based on the derived sensitivity.

2. Formulation

2.1. Equations of state

In this research, the following simple scalar wave equation in the 1D or 2D domain Ω is considered as the equation of state:

$$\frac{\partial^2 U(\mathbf{x},t)}{\partial t^2} = c(\mathbf{x})\nabla^2 U(\mathbf{x},t) \text{ in } \Omega \tag{1}$$

$$U(\mathbf{x},t) = 0 \text{ on } \Gamma_{\mathrm{D}} \tag{2}$$

where U is a scalar function with respect to time and space (representing the height of wave), c is the coefficient function defined in the whole domain and Γ_{D} defines the boundaries on which the Dirichlet condition is imposed with respect to u. The equations correspond to the free vibration of the strings or membranes, axial or torsion vibration of rods, etc. Assuming the time harmonic solution $U(\mathbf{x},t) = e^{-i\omega t}u(\mathbf{x})$ where ω is the frequency and U is the amplitude, the above wave equation is converted into the following Helmholtz equation:

$$-\lambda u(\mathbf{x}) = c(\mathbf{x})\nabla^2 u(\mathbf{x}) \tag{3}$$

$$u(\mathbf{x}) = 0 \text{ on } \Gamma_{\mathrm{D}} \tag{4}$$

where

$$\lambda = \omega^2 \tag{5}$$

where λ is the eigenvalue. For the sensitivity analysis and numerical calculation using the FEM, the variational form of the above equation is also derived as follows:

$$a(u, v) - \lambda b(u, v) = 0 \tag{6}$$

where

$$a(u, v) = \int_\Omega c \nabla u \cdot \nabla v \mathrm{d}x \tag{7}$$

$$b(u, v) = \int_\Omega uv \mathrm{d}x \tag{8}$$

where v is the test function. The solution of the Eqs.(3) or (6) are represented by the infinite family $(\lambda_k, u_k)_{k \geq 1}$. The k-th eigenvalue λ_k is obtained as follows (e.g. Chapter 4 in [40]):

$$\lambda_k = \min_{\substack{u \\ b(u,u_l)=0, \ (l=1,\ldots,k-1)}} \frac{a(u, u)}{b(u, u)} \tag{9}$$

The minimizer of the above k-th equation is the k-th eigenmode u_k.

2.2. Optimization problem

The space dependent function $c(\mathbf{x})$ is regarded as the design variable of the optimization problem. Here we consider the general objective functional calculated from the k-th eigenmode $J(u_k) = \int_\Omega j(u_k) \mathrm{d}x$. We assume that the k-th eigenvalue cannot be the repeated eigenvalue. Introducing the eigenvalue constraint which controls the eigenvalue of the converged solution, the optimization problem is formulated as follows:

$$\underset{c}{\text{minimize}} \, J(c, u_k) = \int_\Omega j(u_k) \mathrm{d}x \tag{10}$$

subject to

$$\lambda_k \leq \lambda_{\max} \tag{11}$$

$$c_{\min} \leq c(\mathbf{x}) \leq c_{\max} \tag{12}$$

and the state equation in Eq.(6) and the normalized condition $|u_k| = 1$, where $\lambda_{\max}$ is the upper bound of the k-th eigenvalue and $c_{\min}$ and $c_{\max}$ are the lower and the upper bound of c.

2.3. Sensitivity analysis

The derivative of the objective function in Eq.(10) with respect to the design variable c is determined. It is performed using the procedure shown in Chapter 5 of [36]. All eigenvalues treated here are assumed not to be repeated.

The derivative of the objective function in Eq.(10) in the direction θ is then:

$$\begin{aligned} \langle J'(c), \theta \rangle &= \int_\Omega j'\left(u_k\right) \langle u_k'(c), \theta \rangle \, \mathrm{d}x \\ &= \int_D j'(u_k) v \mathrm{d}x \end{aligned} \tag{13}$$

where $v = \langle u_k'(c), \theta \rangle$.

Using the weak form of the equations of state in Eq.(6) and introducing the adjoint state p as the test function, the Lagrangian is:

$$L(c, u_k, p) = \int_\Omega j(u_k) \mathrm{d}x + a(u_k, p) - \lambda_k b(u_k, p) \tag{14}$$

Using this, the derivative of the objective function can be expressed as:

$$\begin{aligned} \langle J'(c), \theta \rangle &= \left\langle \frac{\partial L}{\partial c}(c, u_k, p), \theta \right\rangle + \left\langle \frac{\partial L}{\partial u_k}(c, u_k, p), \langle u_k'(c), \theta \rangle \right\rangle \\ &= \left\langle \frac{\partial L}{\partial c}(c, u_k, p), \theta \right\rangle + \left\langle \frac{\partial L}{\partial u_k}(c, u_k, p), v \right\rangle \end{aligned} \tag{15}$$

We consider the case where the second term is zero. It is calculated as follows:

$$\left\langle \frac{\partial L}{\partial u_k}(c, u_k, p), v \right\rangle = \int_\Omega j'(u_k) v \mathrm{d}x + a(v, p) - \left\langle \frac{\partial \lambda_k}{\partial u_k}, v \right\rangle b(u_k, p) - \lambda_k b(v, p) = 0 \tag{16}$$

When u_k is normalized as $b(u_k, u_k) = 1$, the derivative of λ_k with respect to u_k is calculated as follows from Eq.(9):

$$\left\langle \frac{\partial \lambda_k}{\partial u_k}, v \right\rangle = 2a(u_k, v) - 2\lambda_k b(u_k, v) \tag{17}$$

Since this equation equals the equations of state, it becomes zero. Thus, Eq.(16) is simplified as follows:

$$\int_\Omega j'(u_k) v \mathrm{d}x + a(v, p) - \lambda_k b(v, p) = 0 \tag{18}$$

In the case that the adjoint state p satisfies the above adjoint equation, the second term of Eq.(15) can be ignored. On the other hand, the derivative of Eq.(6) about the k-th eigenvalue with respect to c in the direction θ is:

$$\begin{aligned} &\int_\Omega \nabla u_k \cdot \nabla p \theta \mathrm{d}x + a(\langle u_k'(c), \theta \rangle, p) - \langle \lambda_k'(c), \theta \rangle b(u_k, p) - \lambda_k b(\langle u_k'(c), \theta \rangle, p) \\ =& \int_\Omega \nabla u_k \cdot \nabla p \theta \mathrm{d}x + a(v, p) - \langle \lambda_k'(c), \theta \rangle b(u_k, p) - \lambda_k b(v, p) = 0. \end{aligned} \tag{19}$$

The derivative of λ_k with respect to c in the direction θ is calculated as follows:

$$\begin{aligned} \langle \lambda_k'(c), \theta \rangle &= \left\langle \frac{\partial \lambda_k}{\partial c}, \theta \right\rangle + \left\langle \frac{\partial \lambda_k}{\partial u_k}, v \right\rangle \\ &= \int_\Omega \nabla u_k \cdot \nabla u_k \theta \mathrm{d}x \end{aligned} \tag{20}$$

Thus, Eq.(19) becomes:

$$\int_\Omega \nabla u_k \cdot \nabla p \theta \mathrm{d}x + a(v, p) - b(u_k, p) \int_\Omega \nabla u_k \cdot \nabla u_k \theta \mathrm{d}x - \lambda_k b(v, p) = 0. \tag{21}$$

Comparing this equation with Eq.(18), the following is obtained:

$$\int_\Omega j'(u_k)v\mathrm{d}x + \int_\Omega \nabla u_k \cdot \nabla p\theta \mathrm{d}x - b(u_k, p)\int_\Omega \nabla u_k \cdot \nabla u_k \theta \mathrm{d}x = 0 \tag{22}$$

Substituting Eq.(22) into Eq.(13), the derivative of the objective function is:

$$J'(c) = \nabla u_k \cdot \nabla p - b(u_k, p)\nabla u_k \cdot \nabla u_k \tag{23}$$

3. Problem definition

3.1. Definition of the analysis model and optimization problem

We consider the free vibration problems of a 1D string and a 2D membrane. The coefficient c in Eq.(3) is represented as $c = \frac{T}{\rho}$, where T is the tension and ρ is the line density of the string or area density of the membrane. Thus, the optimization problem of the distribution of c is regarded as the mass distribution problem of the string or membrane having uniform tension. Although a non-homogeneous mass distribution with uniform tension is difficult to implement in actual devices, this interpretation is helpful in understanding the mechanical aspect of the optimal results in this problem. Here, as the optimization problem, the eigenmode matching problem is considered. The objective function is formulated as the least squared error (i.e., difference) between the target eigenmode u_0 and the k-th eigenmode u_k as follows:

$$J_1(c) = \sqrt{\int_\Omega (u_k - u_0)^2 \mathrm{d}x}. \tag{24}$$

The k-th and target eigenmodes are both assumed to be normalized. That is, $b(u_k, u_k) = b(u_0, u_0) = 1$ is satisfied.

3.2. Derivation of sensitivity and the adjoint equation

To derive the sensitivity of the objective function $J_1(c)$ in Eq.(24) within the framework described in Section 2.3, the objective function $J(c)$ is redefined as

$$J(c) = \int_\Omega (u_k - u_0)^2 \mathrm{d}x \tag{25}$$

It follows that the derivative of $J_1(c)$ is

$$J_1'(c) = \frac{1}{J_1(c)} J'(c) \tag{26}$$

$J'(c)$ is obtained as a function of the k-th eigenvector u_k and the adjoint state p in Eq.(23). Substituting Eq.(25) into Eq.(18), the adjoint equation is obtained as follows:

$$2\int_\Omega (u_k - u_0) v \mathrm{d}x + a(v,p) - \lambda_k b(v,p) = 0 \tag{27}$$

Note that the k-th eigenvalue λ_k is independent of the adjoint state p. Eq.(27) can be regarded as a linear static problem. The first term can be deemed to be a body force term whose magnitude depends on the error between the current value and the target value. The second term represents the Neumann boundary condition or spring boundary condition on the space whose spring constant is the k-th eigenvalue. That is, the value of the adjoint state becomes larger at the point where the error between the current and the target state is larger.

4. Numerical examples

The following numerical examples are provided to confirm the validity of the proposed method. Figure 1 shows the 1D string and 2D membrane

analysis models. For simplicity, all physical values are treated as being dimensionless. The state and adjoint equations are solved using the FEM from the commercial software of COMSOL Multiphysics [37]. The minimum and maximum values of c, $c_{\min}$ and $c_{\max}$ are respectively set to 10^{-3} and 1 to avoid a singularity. All finite elements are formulated as second order Lagrange elements. Note that we did not encounter the repeated eigenvalue problem [41] or localized mode problem [6] in any numerical example.

Figures 1 is about here.

When the distributions of the design variable are uniform in these domains the first and second eigenmodes are obtained as shown in Fig.2. In these calculations, the 1D and 2D domains are respectively discretized by 100 line elements and 100×80 square elements.

Figure 2 is about here.

For the 1D problem, the target eigenmodes are set to the following two patterns:

For the first mode optimization:

$$u_0 = 0.8304 \times \mathrm{e}^{x} \sin(\pi x) \tag{28}$$

For the second mode optimization:

$$u_0 = \begin{cases} 0.8304 \times \mathrm{e}^{2x} \sin(2\pi x) \text{ for } 0 \leq x < 0.5 \\ 0.8304 \times \mathrm{e}^{2-2x} \sin(2\pi x) \text{ for } 0.5 \leq x \leq 1 \end{cases} \tag{29}$$

For the 2D problem, the target eigenmodes are set as follows:

For the first mode optimization:

$$u_0 = 0.6899 \times \mathrm{e}^x \mathrm{e}^y \sin(\pi x) \sin(\pi y) \tag{30}$$

For the second mode optimization:

$$u_0 = \begin{cases} 1.1759 \times \mathrm{e}^{2x} \sin(2\pi x) \sin(\pi y) \text{ for } 0 \leq x < 0.5 \\ 1.1759 \times \mathrm{e}^{2-2x} \sin(2\pi x) \sin(\pi y) \text{ for } 0.5 \leq x \leq 1 \end{cases} \tag{31}$$

The coefficients are added to normalize u_0. That is, the above target values satisfy $\int_\Omega u_0^2 \mathrm{d}x = 1$ as well as u_k. Eqs.(28) and (30), and Eqs.(29) and (31) are used to optimize the first and the second eigenvalues respectively. These functions are plotted in Fig.3.

Figure 3 is about here.

4.1. Validation of sensitivity analysis

The validity of the analytical sensitivity derived in Eq.(23) was established by comparing the results with sensitivities obtained using the finite difference method (FDM). The analytical sensitivity and the objective function required to calculate the FDM based sensitivity are obtained using the FEM. The FDM is performed according to following equation:

$$J'(c_i) = \frac{J(\mathbf{c} + \mathbf{a}_i \Delta c) - J(\mathbf{c})}{\Delta c}, \ (i = 1, ..., n) \tag{32}$$

where

$$\mathbf{c} = [c_1, ..., c_i, ...c_n] \tag{33}$$

where n is the number of design variables, $\mathbf{a}_i$ is a vector whose i-th element is 1 and other elements are 0, and Δc is set to 10^{-3}. The design variable c is discretized and set for each finite element. The 1D domain is discretized by 100 line elements and the 2D domain is discretized by 50×40 square elements. In the 1D and 2D models, the design variable c is set uniformly to 0.5.

Figure 4 shows comparison results for the 1D problem. Analytical sensitivities are plotted using the curve and numerical sensitivities are plotted using the points at the center of each finite element. Both sets of data were normalized by dividing the values of each vector set by the maximum absolute value for that vector set. The curve of analytical sensitivity coincided with the discrete plot of the numerical sensitivities in both the first and second eigenmodes.

Figure 4 is about here.

Figure 5 shows comparison results for the 2D problem. All sensitivities are represented as distributions in grayscale after normalization. The distributions are almost the same and the validity of the sensitivity analysis is confirmed even in the 2D case.

Figure 5 is about here.

4.2. Optimization examples

In the optimization examples, the design variable is updated by the method of moving asymptotes (MMA) [42] according to the algorithm shown in Fig.6.

Figure 6 is about here.

4.2.1. Examples of unconstrained optimization

As a first numerical study of the optimization, they are performed without any constraints with the 1D problem for the first and second eigenmodes and the 2D problem for the first eigenmode. The same analysis models are used in this study as those used in the sensitivity analysis subsection. Finite element analysis was first performed with 100 line elements in the 1D problem and with 50×40 square elements in the 2D problem. Figures 7 and 8 show the optimal distribution of c, the first order eigenmode u_1 and the history of the objective function and the first order eigenvalue of the 1D and 2D problems respectively. In both results, the obtained eigenmodes achieved good approximations to the target eigenmodes. Since any constraints were not introduced in this calculation, the optimal results were regarded as local optima close to the initial shape and the eigenvalue varied significantly during optimization in the first eigenmode optimization. In the second mode optimization, although the objective function grew in value during the optimization owing to the unexpected discontinuous change of the eigenmode, the solution finally converged. Regarding the distribution of c as the inverse

of the distribution of the mass, the optimal solutions have lower mass at the peak of the target shape. In the other part, the mass varies according to the curvature of the target shape. That is, the curve becomes less steep because of the gradual increase in mass in that part.

Figures 7 and 8 are about here.

As shown in Figs.7 and 8, the optimal distribution of c did not have a smooth shape. As observed in the plate thickness optimization in [43], the discretization of the function c could strongly affect the optimal solution. To confirm this, the optimization of the first eigenmode was performed again with different discretization of the design variable and the finite element mesh. In the 1D problem, the optimization was performed with 50 and 200 line elements. In the 2D problem, the optimization was performed with 25×20 and 100×80 square elements. Figures 9 and 10 show the optimal distribution of c and Tables 1 and 2 show the comparison of the objective function. The higher resolution of the design variable achieved better results and improved distribution of c.

Figure 9 is about here.

Table 1: Comparison of the objective functions with different discretization in the 1D problem.

Mesh	50	100	200
Objective function	5.429×10^{-3}	3.524×10^{-3}	2.218×10^{-3}

Figure 10 is about here.

Table 2: Comparison of the objective functions with different discretization in the 2D problem.

Mesh	25×20	50×40	100×80
Objective function	2.326×10^{-2}	7.905×10^{-3}	5.053×10^{-3}

4.2.2. Examples of constrained optimization

As mentioned in the previous example, the eigenmode fitting problem might have some local optima. To specify them, the eigenvalue constraint was introduced here for the first eigenmode optimization problems. In general, when the eigenvalue was constrained to a higher value, the solution space became smaller. The lowest values of the first eigenvalue were set to 6, 7, 8 and 9 in the 1D problem and 14, 16, 18 and 20 in the 2D problem.

Figure 11 and Table 3 show optimal solutions for the 1D problem. When the lowest eigenvalue is 6, the constraint was not active, although above 6 they were active. This means the design space was restricted by a constraint of more than 7. Above the value, the objective function became worse as the constraint became stricter. In the result with the higher constraint, the difference between the resulting eigenmode and the target value were clearly observed. To have a higher eigenvalue under the same tension, the string must be light, and a high gradient of the mass distribution is difficult to realize in this case. This restricts the generation of the smooth curve required in optimization. Figure 12 and Table 4 show optimal solutions for the 2D problem. The same applies to the 2D case.

Figure 11 is about here.

Table 3: Comparison of the objective functions with different constraints for the 1D problem.

Constraints	None	6	7	8	9
Objective function	3.524×10^{-3}	4.931×10^{-3}	1.035×10^{-2}	2.600×10^{-2}	5.933×10^{-3}
Eigenvalue	4.535	6.314	7.033	7.981	8.999

Figure 12 is about here.

Table 4: Comparison of the objective functions with different constraints for the 2D problem.

Constraints	None	14	16	18	20
Objective function	7.905×10^{-3}	7.912×10^{-3}	9.633×10^{-3}	1.572×10^{-2}	3.455×10^{-2}
Eigenvalue	12.055	14.860	16.047	18.000	20.000

5. Conclusions

The continuum sensitivity of the objective function including the eigenmodes of continuum systems governed by the scalar Helmholtz equations was derived in this research. Numerical optimizations for the simple 1D and 2D vibration problems were performed based on the sensitivity. A scalar Helmholtz equation in the 1D or 2D domain was considered. A sensitivity analysis was performed for the general objective function which is a function of the eigenmode. A minimization problem of the least square error of

the first or second eigenvector was set as a sample objective function. The sensitivity and the adjoint equation were derived in continuum form for this objective function. The simple 1D string and 2D membrane vibration problems were set for the numerical examples. The Helmholtz equation and the adjoint equation were numerically solved using the FEM. The sensitivity was calculated using both the state and adjoint state variables. The results were compared with the sensitivity derived using the finite difference method and the validity of the derived sensitivity was illustrated. Finally, some optimization problems were solved based on the derived sensitivity.

Following from the work described in this paper, there are opportunities for further research. The first is the extension of the proposed method to the repeated eigenvalue problem. The proposed formulation cannot be applied to eigenmode optimization with repeated eigenvalues. Different formulation is required in the case of the repeated eigenvalue as reviewed in [41] for eigenvalue optimization. Second, the sensitivity analysis performed in this paper is limited to the scalar Helmholtz equation. By extending the proposed methodology the vector Helmholtz equation version of the vibration equation of linear elastic bodies, could be utilized for the optimization of the vibration resonator. As performed in the existing research on the optimal design of the resonators [25, 26, 27, 28], topology optimization will help to generate the optimal shape.

Acknowledgments

This research was partially supported by a research grant of Fundamental Research Developing Association Shipbuilding Offshore.

[1] N. Olhoff, Maximizing higher order eigenfrequencies of beams with constraints on the design geometry, Journal of Structural Mechanics 5 (2) (1977) 107–134.

[2] N. Olhoff, G. I. N. Rozvany, Optimal grillage layout for given natural frequency, Journal of the Engineering Mechanics Division 108 (5) (1982) 971–975.

[3] M. P. Bendsøe, N. Kikuchi, Generating optimal topologies in structural design using a homogenization method, Computer Methods in Applied Mechanics and Engineering 71 (2) (1988) 197–224.

[4] M. P. Bendsøe, O. Sigmund, Topology Optimization: Theory, Methods, and Applications, Springer-Verlag, Berlin, 2003.

[5] A. R. Diaz, N. Kikuchi, Solutions to shape and topology eigenvalue optimization problems using a homogenization method, International Journal for Numerical Methods in Engineering 35 (7) (1992) 1487–1502.

[6] N. L. Pedersen, Maximization of eigenvalues using topology optimization, Structural and Multidisciplinary Optimization 20 (1) (2000) 2–11.

[7] T. S. Kim, Y. Y. Kim, Mac-based mode-tracking in structural topology optimization, Computers and Structures 74 (3) (2000) 375–383.

[8] G. Allaire, S. Aubry, F. Jouve, Eigenfrequency optimization in optimal design, Computer Methods in Applied Mechanics and Engineering 190 (28) (2001) 3565–3579.

[9] T. S. Kim, J. E. Kim, Y. Y. Kim, Parallelized structural topology optimization for eigenvalue problems, International Journal of Solids and Structures 41 (9-10) (2004) 2623–2641.

[10] S. J. Osher, F. Santosa, Level set methods for optimization problems involving geometry and constraints. i. frequencies of a two-density inhomogeneous drum, Journal of Computational Physics 171 (2001) 272–288.

[11] G. Allaire, F. Jouve, A level-set method for vibration and multiple loads structural optimization, Computer Methods in Applied Mechanics and Engineering 194 (30-33) (2005) 3269–3290.

[12] A. Takezawa, S. Nishiwaki, M. Kitamura, Shape and topology optimization based on the phasefield method and sensitivity analysis, Journal of Computational Physics 229 (7) (2010) 2697–2718.

[13] Q. Xia, T. Shi, M. Y. Wang, A level set based shape and topology optimization method for maximizing the simple or repeated first eigenvalue of structure vibration, Structural and Multidisciplinary Optimization 43 (4) (2011) 473–485.

[14] S. Yamasaki, S. Nishiwaki, T. Yamada, K. Izui, M. Yoshimura, A structural optimization method based on the level set method using a new geometry-based re-initialization scheme, International Journal for Numerical Methods in Engineering 83 (12) (2010) 1580–1624.

[15] B. L. Pierson, A survey of optimal structural design under dynamic constraints, International Journal for Numerical Methods in Engineering 4 (4) (1972) 491–499.

[16] Z. D. Ma, N. Kikuchi, I. Hagiwara, Structural topology and shape optimization for a frequency response problem, Computational Mechanics 13 (3) (1993) 157–174.

[17] G. H. Yoon, Structural topology optimization for frequency response problem using model reduction schemes, Computer Methods in Applied Mechanics and Engineering 199 (25) (2010) 1744–1763.

[18] L. Shu, M. Y. Wang, Z. Fang, Z. Ma, P. Wei, Level set based structural topology optimization for minimizing frequency response, Journal of Sound and Vibration 330 (24) (2011) 5820–5834.

[19] R. L. Fox, M. P. Kapoor, Structural optimization in the dynamics response regime - a computational approach, AIAA Journal 8 (10) (1970) 1798–1804.

[20] S. Min, N. Kikuchi, Y. C. Park, S. Kim, S. Chang, Optimal topology design of structures under dynamic loads, Structural Optimization 17 (2) (1999) 208–218.

[21] B. S. Kang, G. J. Park, J. S. Arora, A review of optimization of structures subjected to transient loads, Structural and Multidisciplinary Optimization 31 (2) (2006) 81–95.

[22] A. R. Diaz, A. G. Haddow, L. Ma, Design of band-gap grid structures, Structural and Multidisciplinary Optimization 29 (6) (2005) 418–431.

[23] S. Nishiwaki, K. Saitou, S. Min, N. Kikuchi, Topological design considering flexibility under periodic loads, Structural and Multidisciplinary Optimization 19 (1) (2000) 4–16.

[24] D. Tcherniak, Topology optimization of resonating structures using simp method, International Journal for Numerical Methods in Engineering 54 (11) (2002) 1605–1622.

[25] Y. Maeda, S. Nishiwaki, K. Izui, M. Yoshimura, K. Matsui, K. Terada, Structural topology optimization of vibrating structures with specified eigenfrequencies and eigenmode shapes, International Journal for Numerical Methods in Engineering 67 (2006) 597–628.

[26] W. He, D. Bindel, S. Govindjee, Topology optimization in micromechanical resonator design, Optimization and Engineering doi:DOI: 10.1007/s11081-011-9139-1.

[27] P. H. Nakasone, E. C. N. Silva, Dynamic design of piezoelectric laminated sensors and actuators using topology optimization, Journal of Intelligent Material Systems and Structures 21 (16) (2010) 1627–1652.

[28] W. M. Rubio, G. H. Paulino, E. C. N. Silva, Tailoring vibration mode shapes using topology optimization and functionally graded material concepts, Smart Materials and Structures 20 (2011) 025009.

[29] R. L. Fox, M. P. Kapoor, Rates of change of eigenvalues and eigenvectors, AIAA Journal 6 (12) (1968) 2426–2429.

[30] R. B. Nelson, Simplified calculation of eigenvector derivatives, AIAA Journal 14 (1976) 1201–1205.

[31] B. P. Wang, Improved approximate methods for computing eigenvector derivatives in structural dynamics, AIAA Journal 29 (1991) 1018–1020.

[32] O. Pironneau, Optimal Shape Design for Elliptic Systems, Springer-Verlag, New York, 1984.

[33] E. J. Haug, K. K. Choi, V. Komkov, Design Sensitivity Analysis of Structural Systems, Academic Press, Orlando, 1986.

[34] J. Sokołowski, J. P. Zolesio, Introduction to Shape Optimization: Shape Sensitivity Analysis, Springer-Verlag, Berlin, 1992.

[35] G. Allaire, Numerical Analysis and Optimization: An Introduction to Mathematical Modelling and Numerical Simulation, Oxford University Press, 2007.

[36] G. Allaire, Conception Optimale De Structures, Springer-Verlag, Berlin, 2007.

[37] Http://www.comsol.com/.

[38] Http://www.openfoam.com/.

[39] A. R. Inzarulfaisham, H. Azegami, Solution to boundary shape optimization problem of linear elastic continua with prescribed natural vibration mode shapes, Structural and Multidisciplinary Optimization 27 (3) (2004) 210–217.

[40] S. H. Gould, Variational Methods for Eigenvalue Problems: An Introduction to the Methods of Rayleigh, Ritz, Weinstein, and Aronszajn, Dover Publications, New York, 1995.

[41] A. P. Seyranian, E. Lund, N. Olhoff, Multiple eigenvalues in structural optimization problems, Structural Optimization 8 (4) (1994) 207–227.

[42] K. Svanberg, The method of moving asymptotes- a new method for structural optimization, International Journal for Numerical Methods in Engineering 24 (2) (1987) 359–373.

[43] G. Cheng, N. Olhoff, An investigation concerning optimal design of solid elastic plates, International Journal of Solids and Structures 16 (1981) 305–323.

List of all figures

1. Analysis models. (a) 1D string (b) 2D membrane
2. The eigenmodes with a uniform design variable. (a) The first and second eigenmodes of the 1D problem (b) The first eigenmode of the 2D problem (c) The second eigenmode of the 2D problem.
3. Target functions. (a) 1D problem (b) The first eigenmode of the 2D problem (c) The second eigenmode of the 2D problem
4. Comparison between analytical and numerical sensitivities in the 1D problem. (a) The first mode (b) The second mode
5. Comparison between analytical sensitivity and numerical sensitivity in the 2D problem. (a) Analytical and (b) Numerical sensitivities of the first mode problem (c) Analytical and (d) Numerical sensitivities of the second mode problem
6. Flow chart of the optimization algorithm.
7. Optimal results in the 1D problem. (a) Distribution of c (c) u_1 and u_0 (e) History of the objective function and λ_1 for the first eigenmode problem. (b) Distribution of c (d) Distribution of u_2 and u_0 (f) History of the objective function and λ_2 of the second eigenmode problem.
8. Optimal results in the 2D problem. (a) Distribution of c (b) Distribution of u_1 (c) History of the objective function and λ_1
9. Optimal results of the 1D problem with different discretizations. (a) 50 mesh (b) 200 mesh
10. Optimal results in the 2D problem with different discretizations. (a) 25×20 mesh (b) 100×80 mesh

11. Optimal results for the 1D problem. (a), (c), (e), (g) Distributions of c with the constraints 6, 7, 8 and 9. (b), (d), (f), (h) Distributions of u_0 and u_1 with the constraints 6, 7, 8 and 9.
12. Optimal results for the 2D problem. (a), (c), (e), (g) Distributions of c with the constraints 14, 16, 18 and 20. (b), (d), (f), (h) Distributions of u_1 with the constraints 14, 16, 18 and 20.

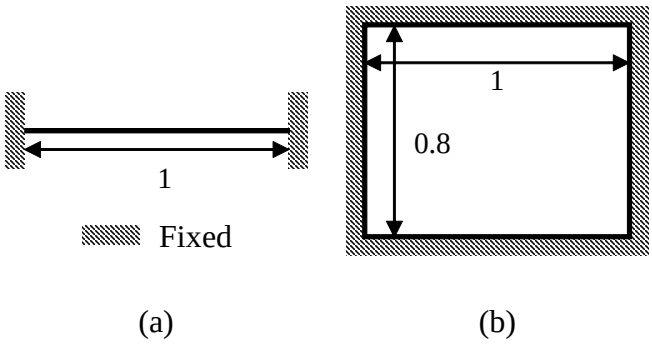

Figure 1: Analysis models. (a) 1D string (b) 2D membrane

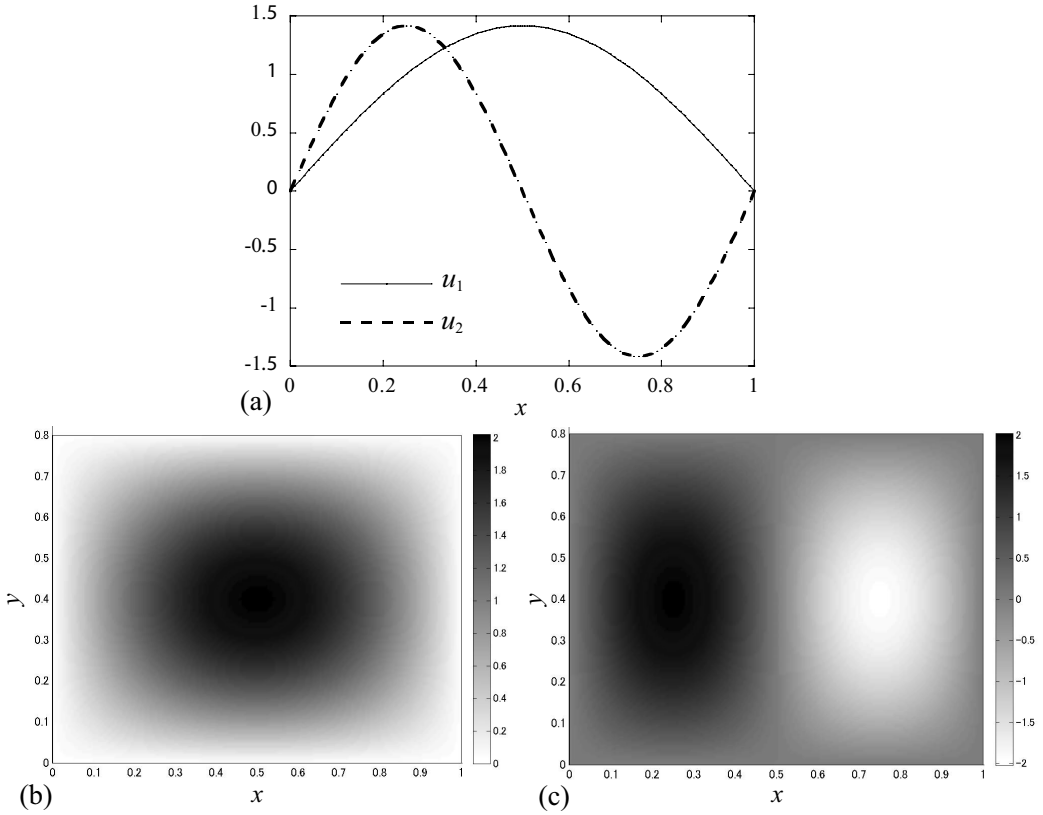

Figure 2: The eigenmodes with a uniform design variable. (a) The first and second eigenmodes of the 1D problem (b) The first eigenmode of the 2D problem (c) The second eigenmode of the 2D problem.

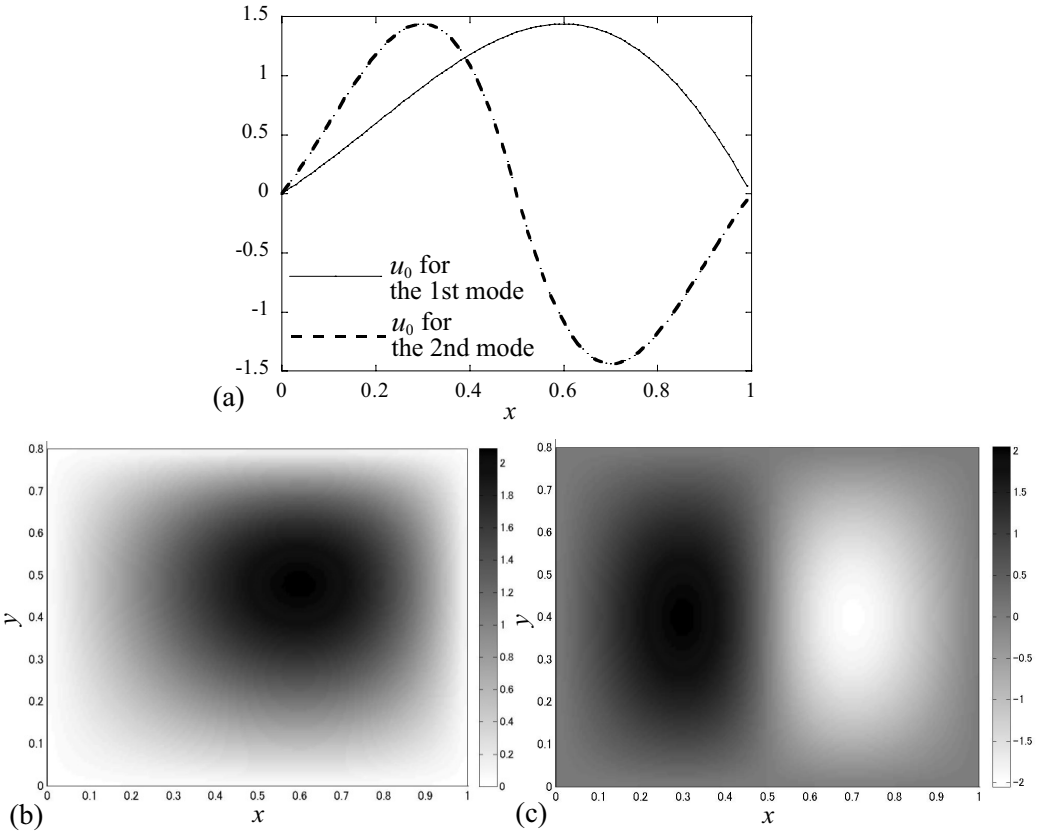

Figure 3: Target functions. (a) 1D problem (b) The first eigenmode of the 2D problem (c) The second eigenmode of the 2D problem

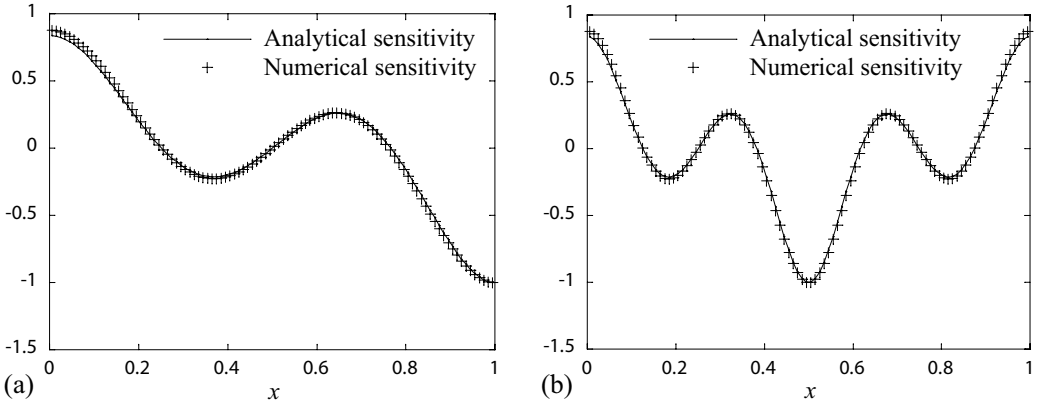

Figure 4: Comparison between analytical and numerical sensitivities in the 1D problem. (a) The first mode (b) The second mode

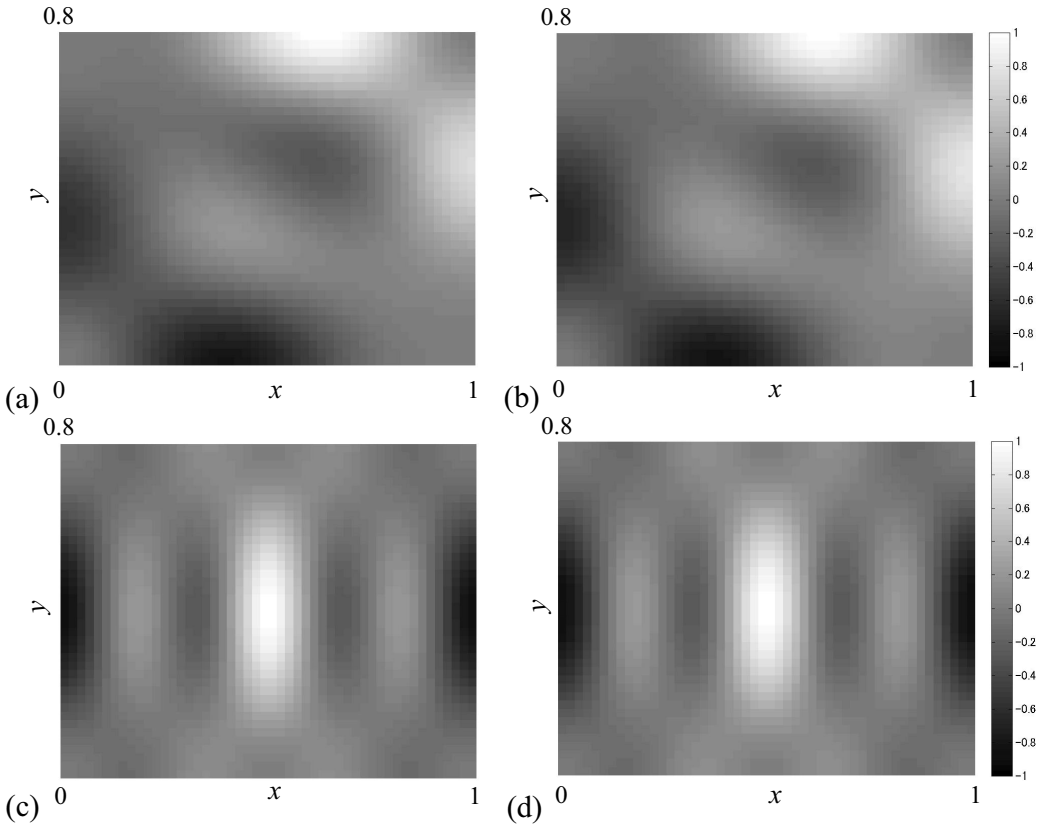

Figure 5: Comparison between analytical sensitivity and numerical sensitivity in the 2D problem. (a) Analytical and (b) Numerical sensitivities of the first mode problem (c) Analytical and (d) Numerical sensitivities of the second mode problem

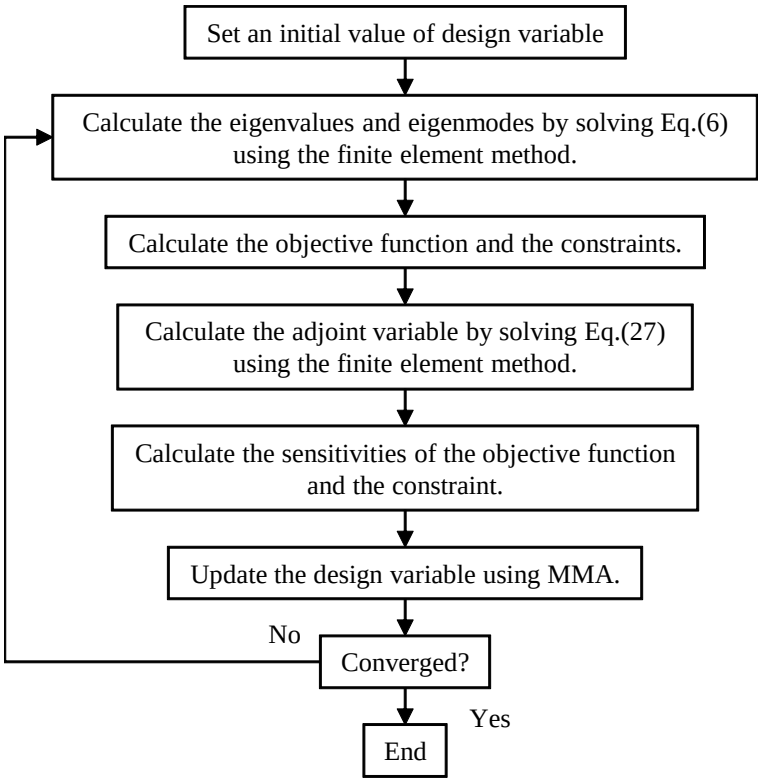

Figure 6: Flow chart of the optimization algorithm.

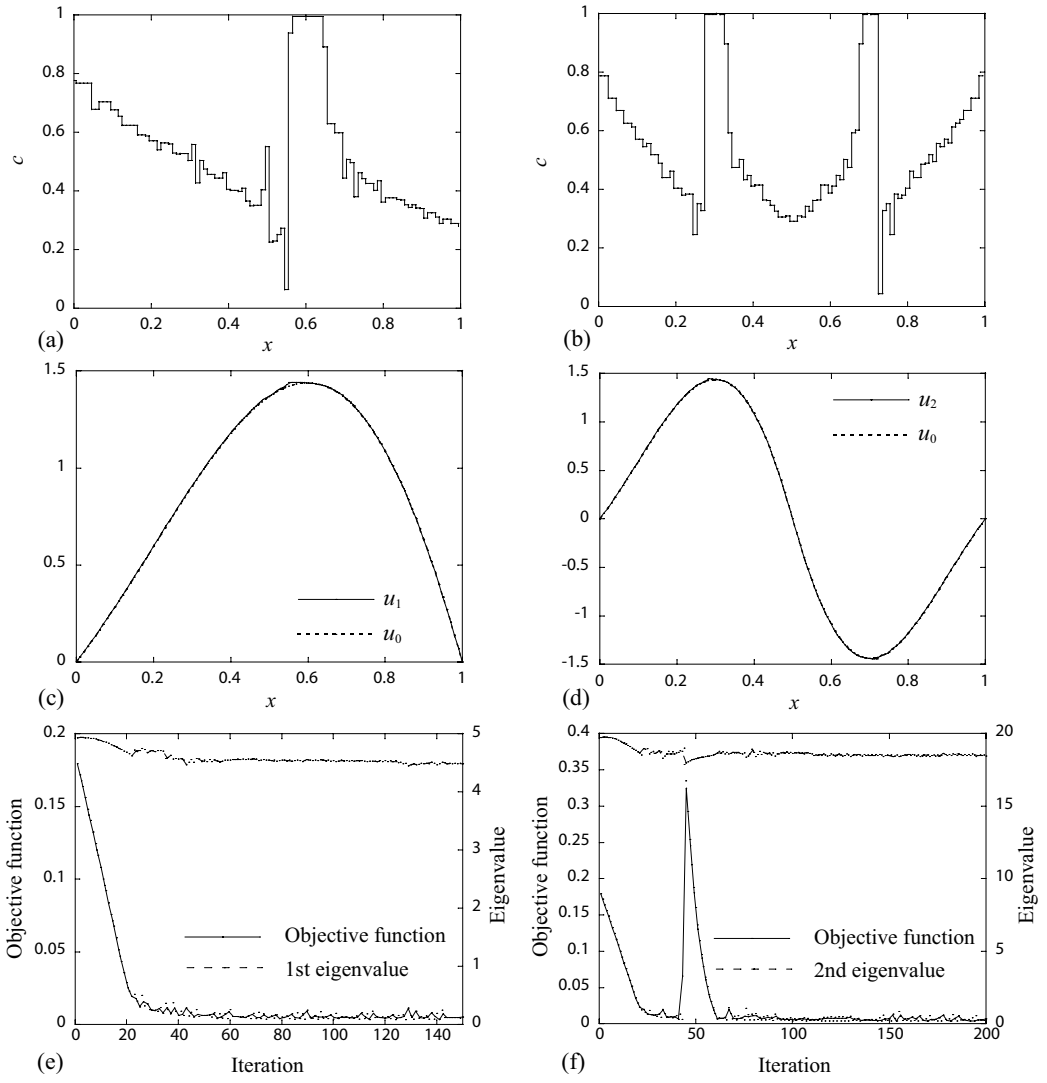

Figure 7: Optimal results in the 1D problem. (a) Distribution of c (c) u_1 and u_0 (e) History of the objective function and λ_1 for the first eigenmode problem. (b) Distribution of c (d) Distribution of u_2 and u_0 (f) History of the objective function and λ_2 of the second eigenmode problem.

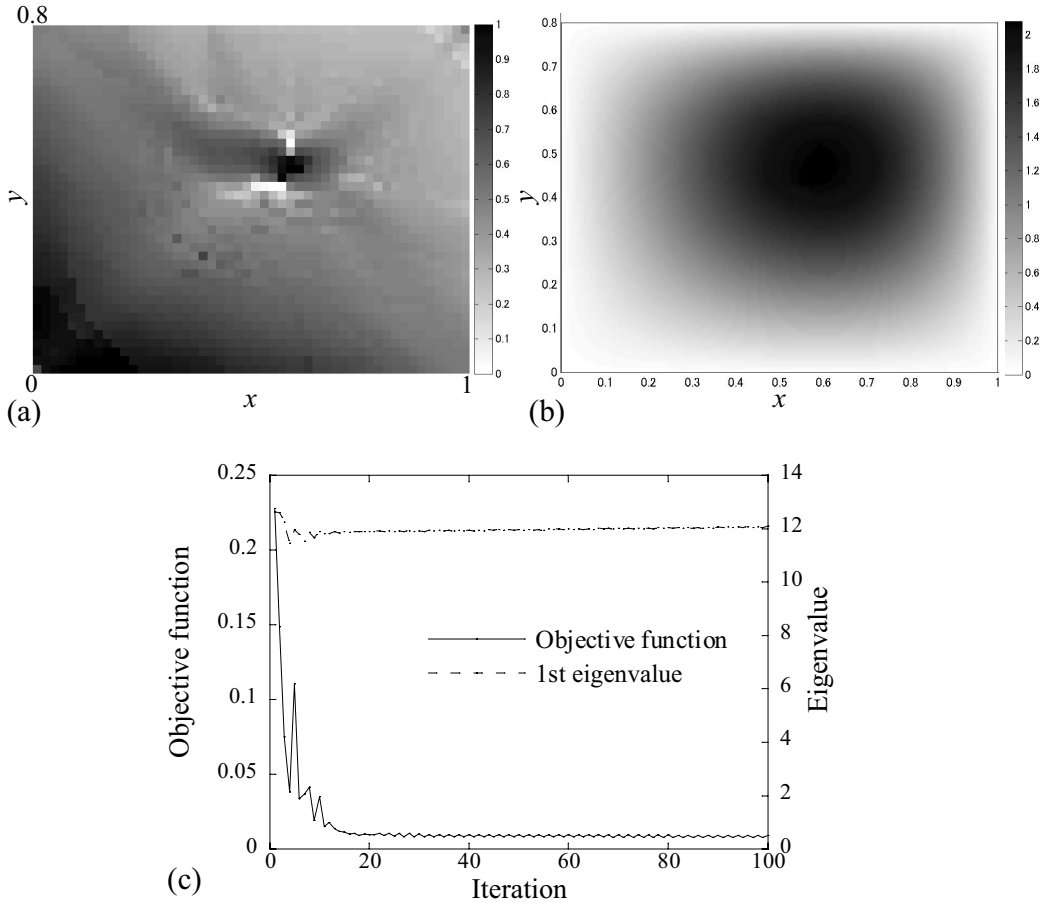

Figure 8: Optimal results in the 2D problem. (a) Distribution of c (b) Distribution of u_1 (c) History of the objective function and λ_1

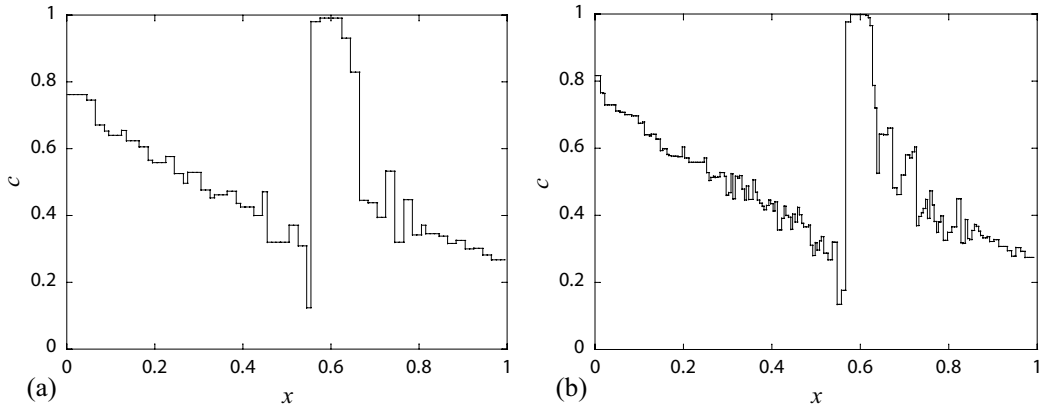

Figure 9: Optimal results of the 1D problem with different discretizations. (a) 50 mesh (b) 200 mesh

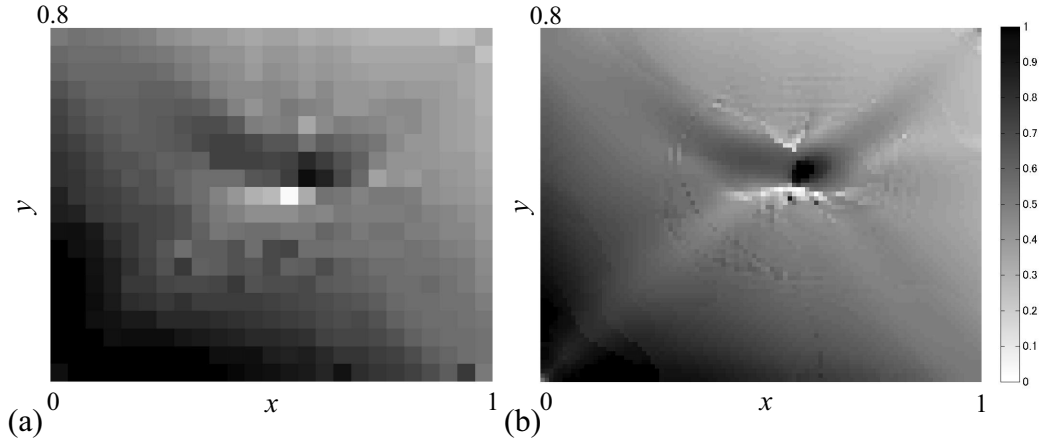

Figure 10: Optimal results in the 2D problem with different discretizations. (a) 25×20 mesh (b) 100×80 mesh

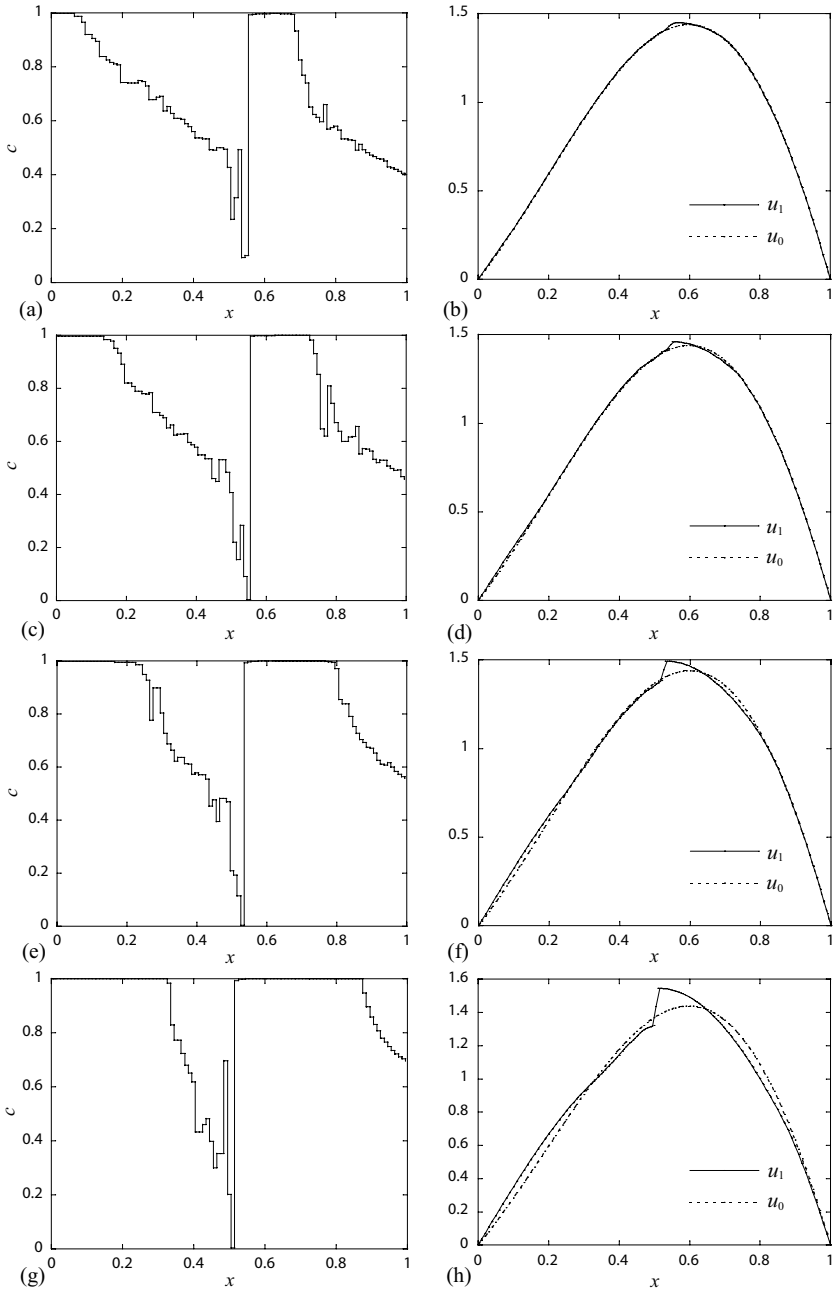

Figure 11: Optimal results for the 1D problem. (a), (c), (e), (g) Distributions of c with the constraints 6, 7, 8 and 9. (b), (d), (f), (h) Distributions of u_0 and u_1 with the constraints 6, 7, 8 and 9.

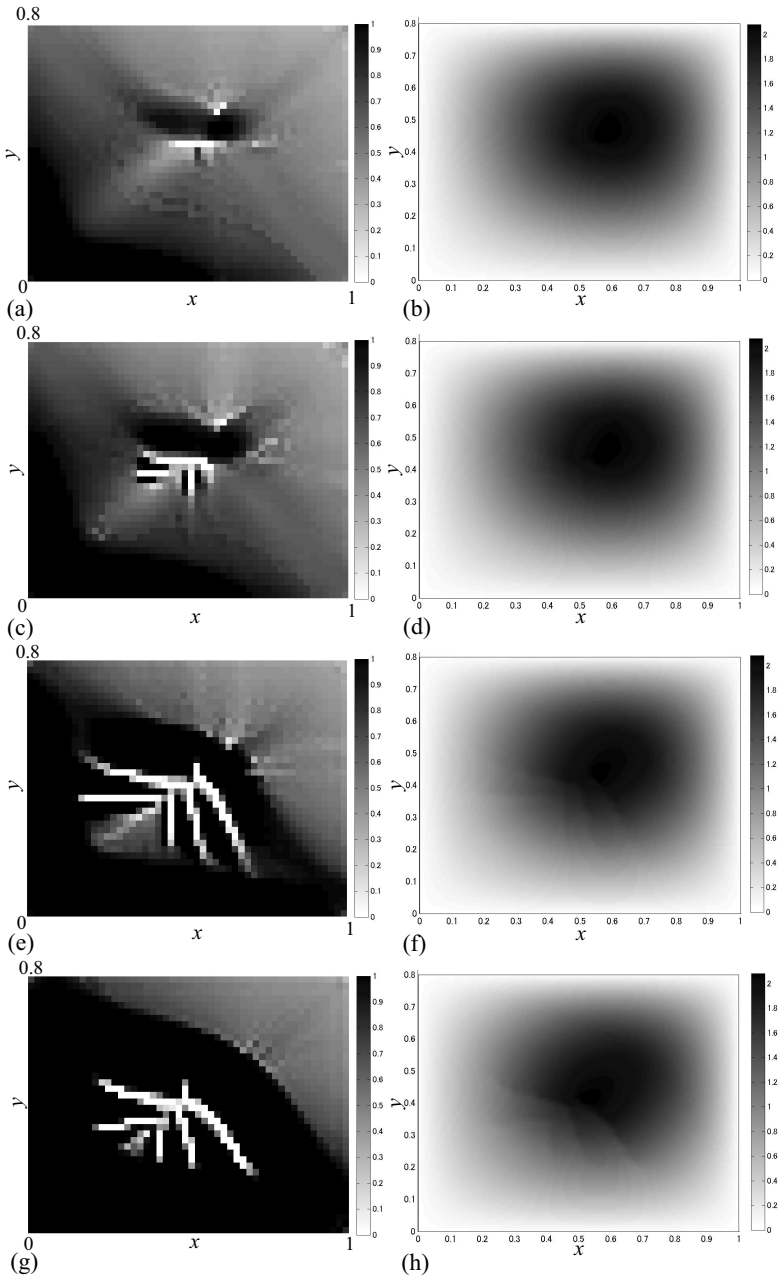

Figure 12: Optimal results for the 2D problem. (a), (c), (e), (g) Distributions of c with the constraints 14, 16, 18 and 20. (b), (d), (f), (h) Distributions of u_1 with the constraints 14, 16, 18 and 20.